

New results from the NA57 experiment

G E Bruno for the NA57 Collaboration †

Dipartimento IA di Fisica dell'Università e del Politecnico di Bari and INFN, Bari, Italy

Abstract. The production of hyperons in Pb-Pb and p-Be interaction at 40 A GeV/ c beam momentum has been measured by the NA57 experiment. Strange particle enhancements at 40 A GeV/ c are presented for the first time and compared to those measured at 158 A GeV/ c . The transverse mass spectra of high statistics, high purity samples of K_S^0 , Λ , Ξ and Ω particles produced in Pb-Pb collisions at 158 A GeV/ c have been studied in the framework of the blast-wave model. The dependence of the freeze-out parameters on particle species and event centrality is discussed.

PACS numbers: 12.38.Mh, 14.20.Jn, 25.75.-q, 25.75.Ld, 25.75.Dw

1. Introduction

The experimental programme with heavy-ion beams at CERN SPS aims at the study of hadronic matter under extreme conditions of temperature, pressure and energy density.

Within this programme, the WA97 experiment has measured an enhanced production of particles carrying one, two and three units of strangeness in central Pb-Pb collisions at 158 A GeV/ c with respect to proton induced reactions at the same energy (Strangeness Enhancement) [1]. The enhancement is defined as the hyperon yield per wounded nucleon in Pb-Pb collisions relative to the yield per wounded nucleon in p-Be collisions, where the number of *wounded nucleons* (N_{wound}) is the number of nucleons which are estimated to undergo at least one primary inelastic collision with another nucleon [2]. The enhancement increases with the strangeness content of the hyperon: Ω s are more enhanced than Ξ s which in turn are more enhanced than Λ s [1]. This pattern was predicted more than 20 years ago as a consequence of Quark Gluon Plasma (QGP) formation [3]. The WA97 results are not reproduced by any conventional hadronic microscopic model.

The assessment of the combined results from a series of heavy-ion experiments suggests indeed that a new state of matter, which features many of the characteristics of the theoretically predicted QGP, is produced in central Pb-Pb collisions at 158 A GeV/ c [4].

NA57 at the CERN SPS is a dedicated second-generation experiment for the study of the production of strange and multi-strange particles in Pb-Pb and p-Be collisions [5]. It continues and extends the study initiated by its predecessor WA97, by (*i*) enlarging the triggered fraction of the inelastic cross-section, thus extending the centrality range

† For the full author list see Appendix “Collaborations” in this volume.

towards less central collisions and *(ii)* collecting data also at lower (40 A GeV/c) beam momentum in order to study the energy dependence of the enhancements.

In this paper we present for the first time results on strangeness enhancements at 40 A GeV/c. The results are then compared with those obtained at 158 A GeV/c.

A detailed study of the transverse mass ($m_T = \sqrt{p_T^2 + m^2}$) spectra for Λ , Ξ^- , Ω^- hyperons, their antiparticles and K_S^0 measured in Pb-Pb collisions at 158 A GeV/c, has been performed. The shapes of the m_T spectra are expected to depend both on the thermal motion of the particles and on the collective flow driven by the pressure. To disentangle the two contributions we rely on the *blast-wave* model [6, 7], which assumes cylindrical symmetry for an expanding fireball in local thermal equilibrium, testing different hypotheses on the transverse flow profile.

2. Data sample and analysis

The results presented in this paper are based on the analysis of the full data sample collected in Pb-Pb collisions, consisting of 460 M events at 158 A GeV/c and 240 M events at 40 A GeV/c. The analysed sample for p-Be collisions at 40 A GeV/c consists of 110 M events. A separate, smaller sample (60 M events) has also been collected, its analysis is currently on the way to completion. At 158 GeV/c, we use as reference data those collected in p-Be and p-Pb interactions by WA97.

The NA57 apparatus has been described in detail elsewhere [8]. The strange particle signals are extracted by reconstructing the weak decays into final states containing only charged particles, using geometric and kinematic constraints, with a method similar to that used in the WA97 experiment [9]. The invariant mass spectra in p-Be at 40 A GeV/c for $p\pi^-$, $\bar{p}\pi^+$ and $\Lambda\pi^-$ after all analysis cuts are shown in figure 1. Hyperon peaks are well centered at the PDG values [10] with FWHM of about 10 MeV (Λ) and 15 MeV (Ξ^-).

For each particle species we define the fiducial acceptance window using a Monte Carlo simulation of the apparatus, in order to exclude the borders where the systematic errors are more difficult to evaluate. For all hyperons, the acceptance window for particle

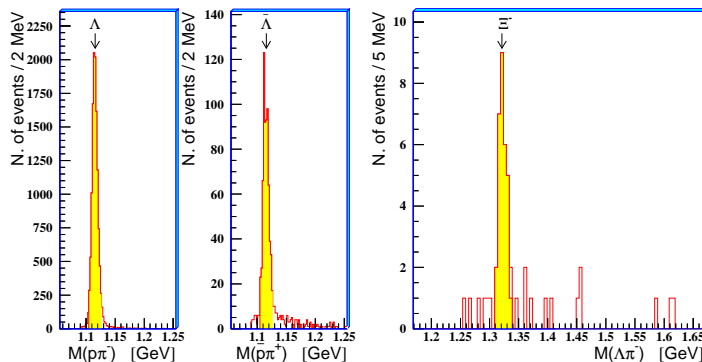


Figure 1. Sample invariant mass spectra for $p\pi^-$, $\bar{p}\pi^+$ and $\Lambda\pi^-$ in p-Be at 40 GeV/c.

and antiparticle are the same, due to the reflection symmetry of our apparatus with respect to the magnetic field direction. As a further check the orientation of the magnetic field was periodically inverted.

All data are corrected for geometrical acceptance and for detector and reconstruction inefficiencies on an event-by-event basis, with the procedure described in reference [11]. It has been checked that the experimental smearings in p_T and y have negligible effects on the weights. The simulation used for calculating the correction factors has been checked in detail (see, e.g., reference [12]) by comparing real and Monte Carlo distributions for the selection parameters.

As a measure of the collision centrality we use the number of wounded nucleons N_{wound} computed via the Glauber model. The procedure for the measurement of the multiplicity distribution and the determination of the collision centrality for each class is described in reference [13]. The distribution of the charged particle multiplicity measured in Pb-Pb interactions has been divided into five centrality classes (0,1,2,3,4), class 0 being the most peripheral and class 4 being the most central. The average N_{wound} in the five centrality classes is given in table 1.

Table 1. Average number of N_{wound} in the five classes defined in Pb-Pb interactions.

0	1	2	3	4
58 ± 4	117 ± 4	204 ± 3	287 ± 2	349 ± 1

3. Strangeness enhancement

The double-differential (y, m_T) distribution for each particle species has been parametrized using the expression

$$\frac{d^2 N}{m_T dm_T dy} = f(y) \exp\left(-\frac{m_T}{T_{app}}\right) \quad (1)$$

assuming the rapidity distribution to be flat within our acceptance region ($f(y) = \text{const}$). By using equation 1 we can extrapolate the yield measured in the selected acceptance window to a common phase space window covering full p_T and one unit of rapidity centered at midrapidity:

$$Y = \int_m^\infty dm_T \int_{y_{cm}-0.5}^{y_{cm}+0.5} dy \frac{d^2 N}{dm_T dy}. \quad (2)$$

The dependence of the K_S^0 , Λ , Ξ and Ω yields on centrality and energy in Pb-Pb collisions has been discussed in a separate contribution to the conference [14]. In p-Be collisions at 40 GeV/c we have measured the yields of Λ , $\bar{\Lambda}$ and Ξ^- . For the Ξ^+ particle, due to the low cross-section and limited statistics, we could estimate only an upper limit to the production yield. This enables us to put an upper limit to the Ξ^+ enhancement.

The enhancement E is defined as

$$E = \left(\frac{Y}{\langle N_{wound} \rangle} \right)_{Pb-Pb} / \left(\frac{Y}{\langle N_{wound} \rangle} \right)_{p-Be} \quad (3)$$

Comparing the measurements at the two beam momenta: for the most central collisions (bins 3 and 4) the enhancements are higher at 40 than at 158 GeV/c, the increase with N_{wound} is steeper at 40 than at 158 GeV/c.

The strangeness enhancement, when described as a consequence of the transition from the canonical to the asymptotic grand canonical limit, is indeed predicted to be a decreasing function of the collision energy [15]. However, that model neither reproduces the steepness nor the amount for central collisions of the measured enhancements.

4. Transverse mass spectra in Pb-Pb at 158 A GeV/c

4.1. Exponential fits

The inverse slope parameter T_{app} (“apparent temperature”) has been extracted by means of a maximum likelihood fit of equation 1 to the data. The apparent temperature is interpreted as due to the thermal motion coupled with a collective transverse flow of the fireball components [6, 7].

The $1/m_T dN/dm_T$ distributions are well described by exponential functions [16]. In the next section, we exploit some small deviations from the exponential in an attempt to disentangle the transverse collective flow from the thermal motion.

The inverse slope parameters T_{app} are given in table 2 as a function of centrality. An increase of T_{app} with centrality is observed in Pb-Pb for Λ , Ξ^+ and possibly also

Table 2. Inverse slopes (MeV) of the m_T distributions for the five Pb-Pb centrality classes (0,4), and for p-Be and p-Pb interactions [17]. Only statistical errors are shown. In Pb-Pb, systematic errors are estimated to be 10% for all centralities.

	p-Be	p-Pb	0	1	2	3	4
K_S^0	197 ± 4	217 ± 6	239 ± 15	239 ± 8	233 ± 7	244 ± 8	234 ± 9
Λ	180 ± 2	196 ± 6	237 ± 19	274 ± 13	282 ± 12	315 ± 14	305 ± 15
$\bar{\Lambda}$	157 ± 2	183 ± 11	277 ± 19	264 ± 11	283 ± 10	313 ± 14	295 ± 14
Ξ^-	202 ± 13	235 ± 14	290 ± 20	290 ± 11	295 ± 9	304 ± 11	299 ± 12
Ξ^+	182 ± 17	224 ± 21	232 ± 29	311 ± 23	294 ± 18	346 ± 28	356 ± 31
$\Omega^- + \bar{\Omega}^+$	169 ± 40	334 ± 99	274 ± 34		274 ± 28	268 ± 23	

for $\bar{\Lambda}$. Inverse slopes for p-Be and p-Pb collisions [17] are also given in table 2. In central and semi-central Pb-Pb collisions (i.e. classes 1 to 4) one observes a baryon-antibaryon symmetry in the shapes of the spectra. This symmetry is not observed in p-Be collisions. The similarity of baryon and antibaryon m_T slopes observed in Pb-Pb suggests that strange baryons and antibaryons are produced by a similar mechanism.

4.2. Blast-wave description of the spectra

The blast-wave model [6] predicts a double differential cross-section of the form:

$$\frac{d^2 N_j}{m_T dm_T dy} = \mathcal{A}_j \int_0^{R_G} m_T K_1 \left(\frac{m_T \cosh \rho}{T} \right) I_0 \left(\frac{p_T \sinh \rho}{T} \right) r dr \quad (4)$$

where $\rho(r) = \tanh^{-1} \beta_{\perp}(r)$ is a transverse boost, K_1 and I_0 are modified Bessel functions, R_G is the transverse geometric radius of the source at freeze-out and \mathcal{A}_j is a normalization constant. The transverse velocity field $\beta_{\perp}(r)$ has been parametrized according to a power law:

$$\beta_{\perp}(r) = \beta_S \left[\frac{r}{R_G} \right]^n \quad r \leq R_G \quad (5)$$

With this type of profile the numerical value of R_G does not influence the shape of the spectra but just the absolute normalization (i.e. the \mathcal{A}_j constant). The parameters which can be extracted from a fit of equation 4 to the experimental spectra are thus the thermal freeze-out temperature T and the *surface* transverse flow velocity β_S . Assuming a uniform particle density, the latter can be replaced by the *average* transverse flow velocity, $\langle \beta_{\perp} \rangle = \frac{2}{2+n} \beta_S$.

The global fit of equation 4 with $n = 1$ to the data points of all the measured strange particle spectra successfully describes all the distributions with $\chi^2/ndf = 37.2/48$, yielding the following values for the two parameters T and $\langle \beta_{\perp} \rangle$:

$$T = 144 \pm 7(\text{stat}) \pm 14(\text{syst}) \text{MeV}, \quad \langle \beta_{\perp} \rangle = 0.381 \pm 0.013(\text{stat}) \pm 0.012(\text{syst}).$$

The T and $\langle \beta_{\perp} \rangle$ parameters are found to be statistically anti-correlated, as can be seen from the confidence level contours shown in figure 3. The systematic errors on T and $\langle \beta_{\perp} \rangle$ are instead correlated; they are estimated to be 10% and 3%, respectively. The use of the three profiles $n = 0$, $n = 1/2$ and $n = 1$ results in similar values of the freeze-out temperatures and of the average transverse flow velocities, with good values of χ^2/ndf . The quadratic profile is disfavoured by our data [16].

It has been suggested (e.g. [18]), based on WA97 results on the hyperon m_T slopes [19] compatible with those of NA57, that the thermal freeze-out occurs earlier for Ω and possibly for Ξ than for particles of strangeness 0, due to the low scattering cross-sections for Ω and Ξ . The 1σ contours of the separate blast-wave fits for singly and multiply strange particles are shown in figure 3. The results of the fits for both groups of particles are compatible with the result of the global fit determination. However, the fit for the multiply strange particles is statistically dominated by the Ξ ; in fact the $\Xi + \Omega$ contour remains essentially unchanged when fitting the Ξ alone.

For the Ω , due to the lower statistics, it is not possible to extract significant values for both freeze-out parameters from its spectrum alone (as can be done for the Ξ). Any possible deviation for the Ω from the freeze-out systematics extracted from the combined fit to the K_S^0 , Λ and Ξ spectra can only be inferred from the integrated information of the Ω spectrum, i.e. from its inverse slope. In figure 3 we plot a compilation of inverse slopes measured in Pb-Pb collisions at 158 A GeV/ c , superimposed to blast-wave model results. The full lines represent the inverse slope one would obtain by fitting an exponential to a ‘‘blast-like’’ $1/m_T dN/dm_T$ distribution for a generic particle of mass m_0 , in the common range $0.05 < m_T - m_0 < 1.50$ GeV/ c^2 , for two different freeze-out conditions: absence of transverse flow ($\langle \beta_{\perp} \rangle = 0$) and our best fit determination. Since the inverse slope is also a function of the $m_T - m_0$ range where the fit is performed, we have also computed

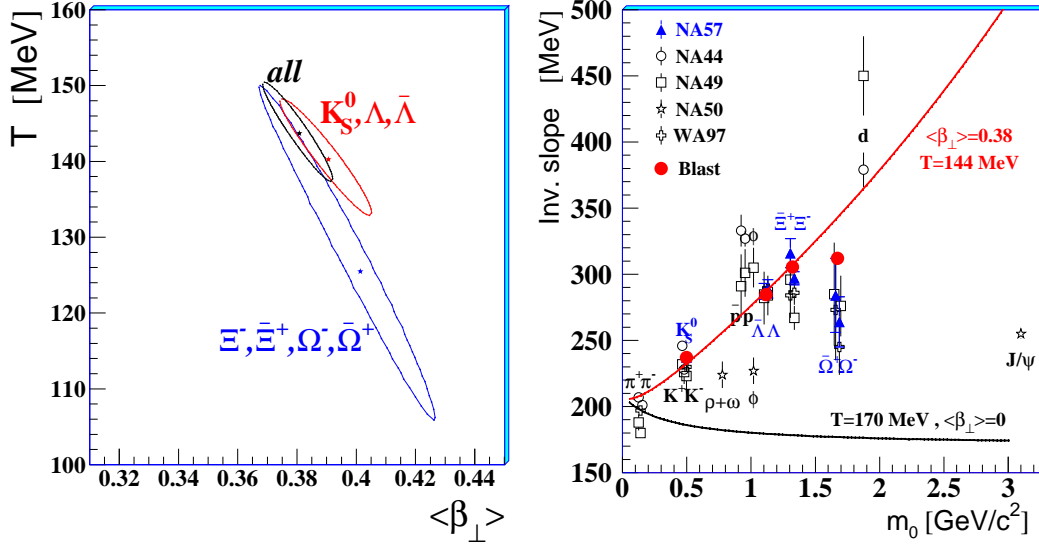


Figure 3. Left: the thermal freeze-out temperature vs the average transverse flow velocity for blast-wave fits using a linear ($n = 1$) velocity profile. The 1σ contours are shown, with the markers indicating the optimal fit locations. Right: prediction of the blast-wave model for inverse slopes (see text for details). For data references see [16].

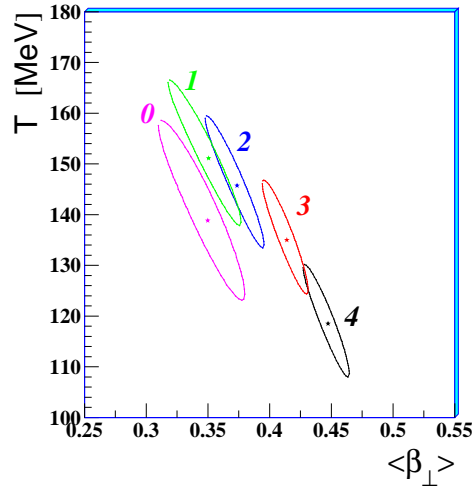


Figure 4. The 1σ confidence level contours from fits in each centrality class.

the blast-wave inverse slopes of K_S^0 , Λ , Ξ and Ω spectra in the $m_T - m_0$ ranges of NA57 (closed circles). The measured values of the inverse slope of the Ω deviate from the blast-wave trend of the other strange particles.

We have also performed the global fit to the spectra for each of the five centrality classes defined in table 1. In figure 4 we show the 1σ confidence level contours as obtained for the $n = 1$ profile. The observed trend is as follows: the more central the collisions the larger the transverse collective flow and the lower the final thermal freeze-out temperature. Higher freeze-out temperatures for more peripheral collisions may be

interpreted as the result of an earlier decoupling of the expanding system.

5. Conclusions

We have reported an enhanced production of Λ , $\bar{\Lambda}$, Ξ^- and $\bar{\Xi}^+$ when going from p-Be to Pb-Pb collisions at 40 A GeV/c. The enhancement pattern follows the same hierarchy with the strangeness content as at 158 GeV/c: $E(\Lambda) < E(\Xi^-)$, $E(\bar{\Lambda}) < E(\bar{\Xi}^+)$. For central collisions (classes 3 and 4) the enhancement is larger at 40 GeV/c. In Pb-Pb collisions the hyperon yields increase with N_{wound} faster at 40 than at 158 A GeV/c.

The analysis of the transverse mass spectra at 158 A GeV/c in the framework of the blast-wave model suggests that after a central collision the system expands explosively and then it freezes-out when the temperature is of the order of 120 MeV with an average transverse flow velocity of about one half of the speed of light. The inverse slope of the Ω particle deviates from the prediction of the blast-wave model tuned on other strange particles (K_S^0 , Λ and Ξ).

Finally, the results on the centrality dependence of the expansion dynamics indicate that with increasing centrality the transverse flow velocity increases and the final temperature decreases.

References

- [1] Andersen E *et al.* 1999 *Phys. Lett. B* **449** 401
Antinori F *et al.* 1999 *Nucl. Phys. A* **661** 130c
- [2] Bialas A, Bleazyński M and Czyż W 1976 *Nucl. Phys. B* **111** 461
- [3] Rafelski J and Müller B 1982 *Phys. Rev. Lett.* **48** 1066
Rafelski J and Müller B 1986 *Phys. Rev. Lett.* **56** 2334
- [4] Heinz U and Jacob M 2000 *Preprint* nucl-th/0002042 and reference therein
- [5] Caliendo R *et al.*, NA57 proposal, 1996 *CERN/SPSLC 96-40, SPSLC/P300*
- [6] Schnedermann E, Sollfrank J and Heinz U 1993 *Phys. Rev. C* **48** 2462
- [7] Schnedermann E, Sollfrank J and Heinz U 1994 *Phys. Rev. C* **50** 1675
- [8] Manzari V *et al.* 1999 *J. Phys. G: Nucl. Phys.* **25** 473
Manzari V *et al.* 1999 *Nucl. Phys. A* **661** 761c
- [9] Andersen E *et al.* 1998 *Phys. Lett. B* **433** 209
Lietava R *et al.* 1999 *J. Phys. G: Nucl. Phys.* **25** 181
Fini R A *et al.* 2001 *J. Phys. G: Nucl. Phys.* **27** 375
- [10] Hagiwara K *et al.* 2002 *Phys. Rev. D* **66** 010001
- [11] Manzari V *et al.* 2003 *Nucl. Phys. A* **715** 140c
- [12] Fanebust K *et al.* 2002 *J. Phys. G: Nucl. Phys.* **28** 160
- [13] Carrer N *et al.* 2001 *J. Phys. G: Nucl. Phys.* **27** 391
- [14] Elia D *et al.* 2004 *J. Phys. G: Nucl. Phys.* , these proceedings
- [15] Tounsi A, Mischke A and Redlich K 2003 *Nucl. Phys. A* **715** 565c
- [16] Antinori F *et al.* 2004 *J. Phys. G: Nucl. Phys.* , in press (*Preprint* nucl-ex/0403016)
- [17] Fini R A *et al.* 2001 *Nucl. Phys. A* **681** 141c
- [18] van Hecke H, Sorge H and Xu N 1998 *Phys. Rev. Lett.* **81** 5764
- [19] Antinori F *et al.* 2000 *Eur. Phys. J. C* **14** 633